Mechanistic modeling of twin screw wet granulation for pharmaceutical formulations: Calibration, sensitivity analysis, and model-driven workflow

Neeru Bala [a], Jeremiah Corrigan [b], Jonathan Meyer [b], Marek Schongut [b], Pankaj Doshi [b], Kiran Iyer [b], Kai Lee [b], Martin Rowland [b], James D. Litster [a], Neil Dawson [b], Rachel M. Smith [a,*]

[a] Department of Chemical & Biological Engineering, University of Sheffield, UK
[b] Pfizer Inc, Sandwich, UK

ARTICLE INFO

ABSTRACT

Wet granulation, a particle size enlargement process, can significantly enhance the critical quality attributes of powders and improve the ability to form tablets in pharmaceutical manufacturing. In this study, a mechanistic-based population balance model is applied to twin screw wet granulation. This model incorporated a recently developed breakage kernel specifically designed for twin screw granulation, along with nucleation, layering, and consolidation. Calibration and validation were performed on Hydrochlorothiazide and Acetaminophen formulations, which exhibit different particle size and wettability characteristics. Utilizing a compartmental experimental dataset, a comprehensive global sensitivity analysis identified critical inputs impacting quality attributes. The study revealed that the nucleation rate process model, effectively represented particle size distributions for both formulations. Adjustments to nucleation and breakage rate parameters, influenced by material properties and screw configuration, improved the model's accuracy. A model-driven workflow was proposed, offering step-by-step guidelines and facilitating PBM model usage, providing essential details for future active pharmaceutical ingredient (API) formulations.

1. Introduction

Twin screw wet granulation has emerged as a key process option for the continuous manufacture of oral solid dosage forms. It involves the use of a twin screw barrel where granulation takes place within a confined space (Thompson, M et al., 2015, Seem, T et al., 2015, Wang, Mustaffar et al., 2017). Twin screw granulation (TSG) can be conceptually divided into zones. Powder is introduced at the barrel's beginning, and liquid addition occurs in the subsequent wetting zone. Rotating screws transport the material through the barrel, facilitating its movement and enabling the formation of granules. This division of zones ensures a controlled and efficient process, where the powder is effectively wetted and mixed with the liquid binder (Saleh et al., 2015). The rotational action of the screws promotes granulation while ensuring binder distribution, mixing and compaction. Overall, TSG optimizes the formation of granules through a well-defined sequence of steps. The process has a short powder residence time, typically less than 30 s, resulting in the formation of strong and porous granules (Wang et al., 2017, El Hagrasy et al., 2020).

In recent years, the pharmaceutical industry has adopted a Quality by Design (QbD) approach, driven by new regulations. QbD focuses on ensuring product quality and minimizing manufacturing costs through good engineering design practices (Litster, 2016). This typically involves the application of data-driven models informed by statistical experimental design (Galvis et al., 2022, Mitchell, 2014). However, applying this approach to Twin Screw Granulation (TSG) can be expensive and inefficient due to the numerous degrees of freedom in the screw configuration, liquid inlet positioning, and process conditions such as screw speed, powder and liquid flow rates and barrel fill level (Van Melkebeke et al., 2008). There is a growing understanding of the mechanistic processes involved in wet granulation, which provides an excellent opportunity to develop useful mechanistic models based on a population balance framework. By incorporating mechanistic models, the experimental burden can be reduced. This alternative approach, referred to as Model Driven Design (MDD), involves using the model to define the design space and conducting targeted experiments to validate the proposed model and estimate key parameters. Mechanistic-based population balance models (PBM) can predict key phenomena within

TSG process, such as under-wetting, by accurately predicting the full particle size distribution (Barrasso et al., 2015, Barrasso & Ramachandran, 2016, Kumar et al., 2016c, Van Hauwermeiren et al., 2019).

In the past, researchers have integrated population balance modeling (PBM) with data-driven techniques like partial least squares (PLS) regression to link PBM outputs with granule quality attributes. For instance, Liu et al, (2019) used PLS regression to relate PBM kernel parameters to TSWG process variables. Barrera Jimenez et al, further enhanced predictive capabilities by connecting material properties and process parameters with PBMs by making advancements include hybrid compartmental models and PLS improving 1D PBMs, and extending to 2D models incorporating consolidation processes (Jiménez et al., 2021, Jiménez et al., 2023a,b). Peeters et al. also developed predictive models based on initial material properties and studied the effect of formulation properties and process settings on granule formation in TSWG at four locations (Peeters et al., 2023, Peeters et al., 2024). This information is crucial for developing predictive mechanistic models like multi-dimensional PBMs (Jiménez et al., 2023c).

However, prior research has encountered significant challenges. Firstly, in integrating rate process kernels tailored to the specific screw configuration in TSG. This is due to the distinct balance of rate processes and the influence of material properties and process parameters that set TSG apart from other wet granulation methods. Secondly, there has been a lack of in-depth understanding regarding uncertainty analysis along the granulator compartments, limiting the applicability of models in decision-making processes within the industry.

By incorporating rate kernels explicitly designed for TSG, it becomes possible to enhance modeling accuracy and facilitate a more thorough investigation of the cause-and-effect relationships between various process and formulation factors, addressing a significant gap observed in prior research. Wang et al., 2020 successfully developed a TSG-specific breakage kernel based on experimental data and applied it effectively in a PBM model for TSG (Wang et al., 2021). However, this study, aimed at exploring the intricate parameter space, was constrained by its approach of conducting only three simulations per parameter—comprising a reference level and variations at specific percentages (local sensitivity analysis). Additionally, the study solely quantitatively evaluated the effects on the D50 of granule size with one type of active material, which was hydrophilic in nature.

This work aim to develop deeper understanding of the TSG process via population balance modeling and by integrating a recently developed breakage kernel, specifically developed for a twin screw wet granulator (Wang et al., 2020), in addition to other previously developed kernels for the remaining key processes: nucleation, layering and consolidation. In this work, the model was calibrated and tested on two different API formulations (hydrophilic and hydrophobic). A comprehensive global systems analysis (Variance-based) was performed for both hydrophobic and hydrophilic formulations to identify which inputs or model parameters have the most significant impact on the output (D10, D50, D90). A compartmental parameter estimation approach was developed based on mechanistic process knowledge of critical parameters and sensitivity analysis. While previous research has primarily focused on overall parameter estimation in twin screw wet granulation (TSWG), our study delves deeper by conducting compartmental parameter estimation and model calibration, targeting specific mechanisms. The utilization of a compartmental parameter estimation approach within the PBM framework, which, to the best of our knowledge, is being employed for the first time, reduces the need for extensive characterization experiments typically required for model optimization in TSG processes. Furthermore, a new model driven workflow is proposed to use the model for the development of twin screw granulation processes, enabling the targeting of key experimental data to parameterize the model, and reducing the traditionally high experimental burden of twin screw granulation process development. This methodology aids understanding of the model parameter space and of interactions between parameters, especially when dealing with diverse nature of active materials. Additionally, this novel step-by-step modeling guideline through a model-driven workflow, can be used as a valuable resource for industry practitioners and engineers engaged in TSWG process development. The application of this model in industry can allow to reduce process development time and costs.

2. Twin screw granulation experiments

2.1. Materials and granulation equipment

Experimental data for the calibration and validation of the model was obtained from Pfizer Inc (Verstraeten et al., 2017). Two formulations were used in the study, each containing a different type of active pharmaceutical ingredient (API). One formulation involved the hydrophobic API Hydrochlorothiazide (HCT), while the other formulation contained hydrophilic API Acetaminophen (APAP). Both formulations incorporated four excipients alongside the API: Lactose monohydrate (Pharmatose 200 M), microcrystalline cellulose (Avicel PH101), croscarmellose sodium (Ac-Di-Sol), and hydroxypropylcellulose (Klucel EF). Experimental data was generated using high shear twin-screw wet granulation module of the ConsiGmaTM-25 system (GEA Pharma systems, Collette, Wommelgem, Belgium). The specific compositions of each formulation is shown in the Table 1 below. Further details regarding the experimental setup and materials can be found in previous publication Verstraeten et al., 2017.

2.2. Design of experiment and data collection

A 3-level full factorial design of experiments was created, where three key process inputs were varied (throughput of powder, screw speed, and liquid-to-solid (L/S) ratio) (Verstraeten et al., 2017). The particle size distribution of the granules produced was measured as the output. This resulted in 27 experiments for each formulation, the specific ranges of process inputs for each formulation are provided in Fig. 1 b) along with additional experiments carried out for validation purposes. Granule samples were collected in well-defined compartments along the length of the granulator unit, as shown in Fig. 1 a). The main objective of the study was to measure the resulting particle size distribution of the granules at different locations as the primary output parameter.

- Compartment 1: Before the first kneading compartment, where granulation liquid is added (wetting zone)
- Compartment 3: After the first kneading compartment
- Compartment 5: After the second kneading compartment
- Compartment 6: After the narrow chopper section (i.e. granulator outlet)

For further details of the experimental conditions and compartments refer to Verstraeten et al., 2017.

3. Population balance model (PBM) for twin screw granulation

A compartmental approach was used to reflect the changing dominant rate processes in the varying zones of the twin screw granulator

Table 1
Compositions for both formulations used (Verstraeten et al., 2017).

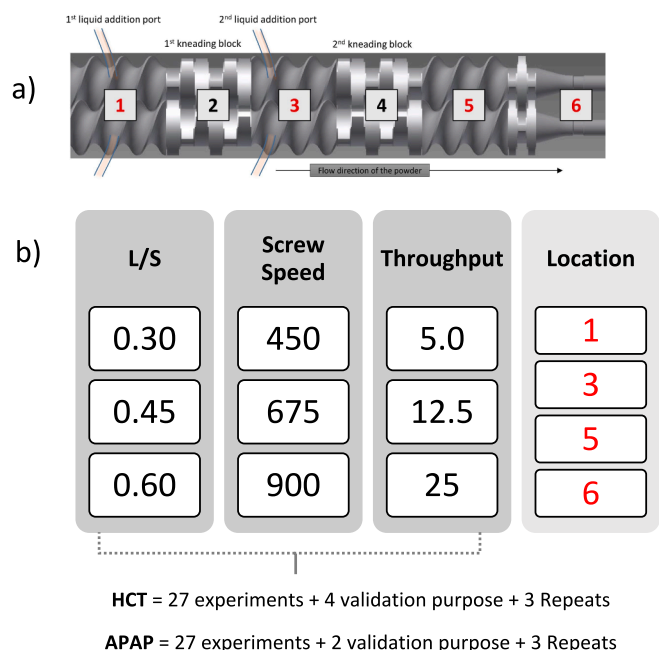| API/Excipient	Concentration (%)	
	HCT Blend	APAP Blend
API	60	60
Pharmatose 200 M (Lactose monohydrate)	16	16
Avicel PH101 (Microcrystalline cellulose)	16	16
Klucel EF (Hydroxypropyl cellulose)	3	3
Ac-Di-Sol (Croscarmellose Sodium)	5	5

Fig. 1. A) sampling in different locations (marked in red) (Verstraeten et al., 2017) b) Overview of different levels of process conditions and number of experiments for the two formulations.

(Barrasso and Ramachandran, 2016, Verstraeten et al., 2017, and Wang et al.,2021). This method entails partitioning every screw configuration into multiple compartments, each representing an individual screw element type. It is postulated that each compartment is thoroughly mixed, and powder and granules move from the preceding (upstream) compartment to the following (downstream) compartment. Additionally, liquid may be introduced to any compartment. A one-dimensional population balance for the granule phase with volume as the internal ordinate is written as:

$$\frac{\partial}{\partial t}n_i(v,t) + \frac{\partial}{\partial v}[n_i(v,t)G_i(v)] = B_{nuc,i}(v,t) + B_{break,i}(v,t) - D_{break,i}(v,t)$$
$$+ \frac{n_i(v) - n_{i-1}(v)}{\tau_i} \tag{1}$$

Where,

v = granule volume, t = time.

$n_i(v,t)$ = granule number density of species i with volume v at time $.t$

$G_i(v)$ = granule growth rate by layering and consolidation

$B_{nuc,i}(v,t)$ = birth rate of new granules due to nucleation

$B_{break,i}(v,t)$ & $D_{break,i}(v,t)$ = birth and death of granules due to breakage.

τ_i = mean residence time.

These rate processes – nucleation, layering, and breakage – are included in the model based on the mechanistic understanding of TSG from literature. In the development of the PBM model in gPROMS Formulated Products v2.2.0 (Siemens Process Systems Enterprise, 2021), selection of relevant rate processes is a critical stage. The key constitutive equations for the included rate kernels are summarized briefly in the below section.

3.1. Rate processes

The availability of different rate process model equations was explored. Breakage is one of the most dominant processes in the twin screw granulator (Wang et al., 2020; Wang et al., 2021), and it is critical to use a kernel developed specifically for the TSG process to improve model performance (El Hagrasy et al., 2013). Therefore, in this work, a recent breakage kernel, specifically developed for a twin screw wet granulator (Wang et al., 2020), was utilized in PBM. Additionally, other previously developed rate kernels for the remaining key processes: nucleation, layering and consolidation were implemented in the model. A summary of the specific models representing each rate process can be found in Table 2.

3.2. Process model configuration and implementation

A concise flowsheet model was implemented in gPROMS formulated products which comprises of series of essential components and considerations. These include careful selection of a material system (API & excipients), utilization of a binder, deliberate choice of relevant rate kernels and sensors, efficient exploration and adjustment of screw configuration aligned with experimental study (Verstraeten et al., 2017). These integrated elements collectively contributed to the accurate and efficient simulation of PBM model and are summarized in the sketch below (Fig. 2).

4. Global sensitivity analysis (GSA)

The primary goal of sensitivity analysis was to identify the relative significance of model inputs and parameters on the output (in this case, D10, D50, D90). This enabled the prioritization of parameter estimation, with greater confidence required for highly sensitive parameters. Previous studies have primarily employed local sensitivity analysis (Wang et al., 2021) or methodologies like elementary effects, which tend to provide only limited quantification of the impact on output changes (Morris, 1991, Campolongo et al., 2005). In this work, a Variance based sensitivity analysis was performed that assessed the contribution of each factor to the variance in a response (Sobol' 2001, Saltelli 2008). This analysis used variance-based metrics to determine how much of the response variance can be attributed to the change in each factor. The main shortcoming of the variance-based sensitivity analysis is its high computational cost, which becomes prohibitive for computationally expensive models. Estimating the sensitivity indices requires a large number of model evaluations. In fact, N*(k + 2) model evaluations are required for each deterministic scenario, where N is the number of probabilistic samples requested and k the number of probabilistic factors. In this study, global sensitivity analysis simulations utilized the following parameter settings for both models: Nucleation: N = 200, K = 3 (total samples = 1000), Layering: N = 170, K = 4 (total samples = 1020) and Breakage: N = 20, K = 9 (total samples = 220). This method distinguishes between first order (main effect contribution of each input factor to the variance of the output) and total effect (accounts for i^{th} factor individual contribution plus all higher-order effects due to its interactions with other factors). Table 3 and 4 represent the results of the sensitivity analysis for the Nucleation, Layering, and Breakage rate processes for to the APAP and HCT model respectively.

In Fig. 3, comparison between two models based on sensitivity analysis of individual rate processes (Nucleation, Layering and Breakage) is shown. The average of total effect Sobol indices across D10, D50 and D90 is shown the plots. Notably, the ranking of parameters remains consistent for the nucleation and layering rate processes across both formulations, indicating their significant influence. A divergence in parameter rankings between two formulations for the breakage rate process is observed based on the total average effect of D10, D50, and D90. However, It is important to highlight that, the parameter's ranking remains very similar when examining the individual total effect of D90 and D50 values. Minor variations in ranking are only observed among the least impacting parameters in each formulation, suggesting a smaller influence on the overall performance of the breakage mechanism. A summary of all model parameters is shown in Table 5.

Table 2

Summary of rate processes used in the population balance model of TSWG.

| Mechanism	Model Equation	Category
Nucleation	Barrasso and Ramachandran, 2015	Semi-mechanistic
	$$f\left(\mu_{drop}\right) = \frac{1}{\mu_{drop}} \frac{1}{\sigma_{drop}\sqrt{2\pi}} exp\left(\frac{\left(\ln\mu_{drop} - \mu_{drop,mean}\right)^2}{2\sigma_{drop}^2}\right) \quad (2)$$	
	$f\left(\mu_{drop}\right)$ = probability density function,	
	μ_{drop} = Drop size	
	$\mu_{drop,mean}$ = Mean droplet size	
	σ_{drop} = Standard deviation	
Breakage	Wang and Pradhan et al., 2020	Mechanistic
	$B_{break,i}(v,t) - D_{break,i}(v,t) = \int_v^\infty S_i(w)b_i(w,v)n_i(w,t)dw - S_i(v)n_i(v,t) \quad (3)$	
	$S_i(v) = S_{o,i}P_{b,i}(v)$	
	$B_{break,i}(v,t)$	
	$D_{break,i}(v,t)$ = birth and death of granules due to breakage.	
	$S_i(v), S_i(w)$ = Specific breakage rates of granules of volume v and w in compartment i	
	$b_i(w,v)$ = fragment size distribution of breakage of granule of volume w in compartment i	
	$S_{o,i}$ = breakage rate constant	
	$P_{b,i}(v)$ = probability of breakage of a granule of volume v	
Layering	Cameron et al., 2005 $G = G_m\frac{M_{powder}}{kM_{granulate} + M_{powder}} exp\left[-\alpha(x_w - x_{wc})^2\right] \quad (4) G_m$ = Maximum growth rate	Mechanistic
	M_{powder} = Mass of powder	
	$M_{granulate}$ = Mass of granules	
	x_w = Moisture content	
	x_w = Critical moisture content	
	$k \& \alpha$ = adjustable kinetic parameters	
Consolidation	Iveson et al., 1996	Empirical
	$R_i(\varepsilon) = -k_i(\varepsilon_i - \varepsilon_{min}) \quad (5)$	
	R_i = Rate of Consolidation,	
	ε_i = Porosity ε_{min} = minimum porosity, k_i = Consolidation rate constant	
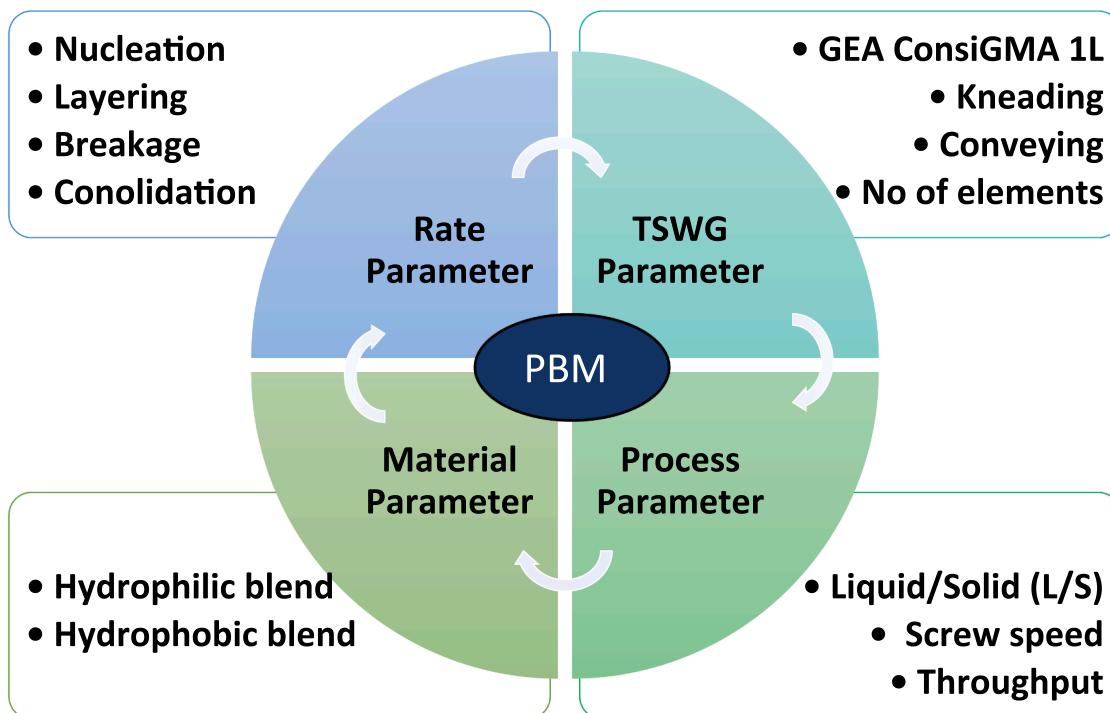
Fig. 2. The category of input parameters in PBM model.

5. Results and discussion

5.1. Minimizing experimental design for model calibration

Understanding the magnitude of the effect of each of the process inputs on the output is necessary to aid in creating the minimal exper-imental design for model calibration. Several studies demonstrate the effects process inputs in the TSG have on the critical quality attributes, such as the granule particle size. These studies show that L/S ratio is the most significant process variable, followed by throughput and then screw speed (Dhenge et al., 2012, Vanhoorne et al., 2016, Verstraeten et al., 2017). The powder feed number (PFN), often also represented by

Table 3

APAP GSA for Nucleation, Layering and Breakage parameters in the TSG PBM.

Rate process	Parameters	D10		D50		D90	
		First Order	Total Effect	First Order	Total Effect	First Order	Total Effect
Nucleation	Droplet pore penetration	1.00	1.09	0.75	0.92	0.66	0.70
	Mean droplet diameter	0.00	0.00	0.09	0.19	0.28	0.34
	St. dev. of droplet diameter	0.00	0.00	0.06	0.13	0.01	0.01
Layering	Kinetic parameter K	0.00	1.58	0.48	1.04	0.41	1.13
	Critical moisture content	0.00	0.87	0.00	0.34	0.00	0.38
	Layering rate constant	0.00	0.38	0.00	0.29	0.00	0.31
	Kinetic parameter A	0.00	0.05	0.00	0.06	0.00	0.06
Breakage	Breakage Rate Constant − Kneading	0.00	0.13	0.00	0.28	0.44	1.25
	Shape − Kneading	0.00	0.75	0.00	2.78	0.00	0.24
	Breakage Rate Constant − Conveying	0.00	0.17	0.00	0.02	0.00	0.19
	Critical Particle Size − Kneading	0.00	0.03	0.00	0.07	0.00	0.06
	Scale − Kneading	0.00	0.12	0.00	0.08	0.00	0.04
	Dynamic Yield Strength	0.00	0.02	0.00	0.01	0.00	0.001
	Fraction of Fines − Conveying	0.00	0.57	0.00	0.04	0.00	0.00
	Critical Particle Size − Conveying	0.00	0.002	0.00	0.00	0.00	0.00
	Fraction of Fines − Kneading	0.00	0.00	0.00	0.00	0.00	0.00

Table 4

HCT GSA for Nucleation, Layering and Breakage parameters in the TSG PBM.

Rate process	Parameters	D10		D50		D90	
		First Order	Total Effect	First Order	Total Effect	First Order	Total Effect
Nucleation	Droplet pore penetration	0.97	1.07	0.67	0.91	0.53	0.55
	Mean droplet diameter	0.00	0.01	0.08	0.23	0.41	0.44
	St. dev. of droplet diameter	0.00	0.01	0.03	0.18	0.02	0.04
Layering	Kinetic parameter K	0.00	1.31	0.12	1.23	0.17	1.22
	Critical moisture content	0.00	0.67	0.00	0.57	0.00	0.56
	Layering rate constant	0.00	0.29	0.00	0.28	0.00	0.28
	Kinetic parameter A	0.00	0.06	0.00	0.07	0.00	0.07
Breakage	Breakage Rate Constant − Kneading	0.13	0.04	0.00	0.04	0.30	0.92
	Shape − Kneading	0.08	0.03	0.09	0.40	0.00	0.21
	Breakage Rate Constant − Conveying	0.24	0.12	0.00	0.17	0.00	0.21
	Dynamic Yield Strength	0.26	0.33	0.00	0.44	0.00	0.11
	Critical Particle Size − Conveying	0.12	0.19	0.28	0.70	0.00	0.09
	Scale − Kneading	0.08	0.00	0.00	0.01	0.00	0.04
	Critical Particle Size − Kneading	0.11	0.00	0.00	0.01	0.00	0.04
	Fraction of Fines − Conveying	0.34	0.38	0.00	0.07	0.00	0.02
	Fraction of Fines − Kneading	0.10	0.00	0.00	0.00	0.00	0.00

"fill level", has been documented as a key variable that can capture the interactions between throughput and screw speed as shown below, and may be more useful than considering those variables independently (Osorio et al., 2017, Meier et al., 2017, Gorringe et al., 2017, Kumar et al., 2016a-c).

$$PFN = \frac{\dot{m}_{powder}}{\rho_{bulk}\omega D^3} \tag{6}$$

Where, $\dot{m}_{powder}$ is throughput, ω is screw speed, ρ_{bulk} is bulk density of powder and D diameter of screw. Kumar et al. (2016c) noted that the effect of L/S on granule particle size distribution is most evident at higher PFN (lower screw speed/higher throughput). Considering this effect of PFN, it seems unnecessary to vary both screw speed and throughput within an experiment design to capture the most variation within the particle size, particularly when looking to minimise costs and material resources associated with experimentation. In this work a method is proposed to minimise the number of experiments required for model calibration, while capturing this variation in granule size. In this method, high and low PFN values are used for each L/S ratio considered. In this work, this would involve 2 PFN levels for each of the 3 L/S ratios, giving a total of 6 experiments for model parameter estimation (Fig. 4).

5.2. Parameter estimation and model validation

Experimental data from Verstraeten et al. (2017) was used for parameter estimation and validation of the model. Granule samples were collected in well-defined compartments along the length of the granulator unit in their study. In Fig. 5, an approach for parameter estimation is illustrated. The selection of compartments for parameter estimation was based on the dominance of specific rate processes. For example, since nucleation is primarily dominant in the wetting zone (Compartment 1), the nucleation-related parameters were estimated using data collected specifically from Compartment 1. This was followed by the estimation of layering and breakage parameters using data from Compartment 3, with the nucleation parameters updated based on the estimation in the previous compartment (wetting zone). The parameter estimation process can be summarized as follows:

- Step 1: Estimate nucleation parameters using data from Compartment 1, without considering layering, breakage, consolidation.
- Step 2: Estimate layering and breakage parameters using data from Compartment 3, while updating the nucleation parameters obtained in Step 1.
- Step 3: Validate the model using data from Compartment 5.
- Step 4: Further validation of the model using data from Compartment 6.

Given only two narrow kneading elements between compartment 5 and compartment 6, we prioritize on discussing results from the granulator outlet (L6), a key focus in the majority of granulation studies. When discussing granule size distribution in the sections below,
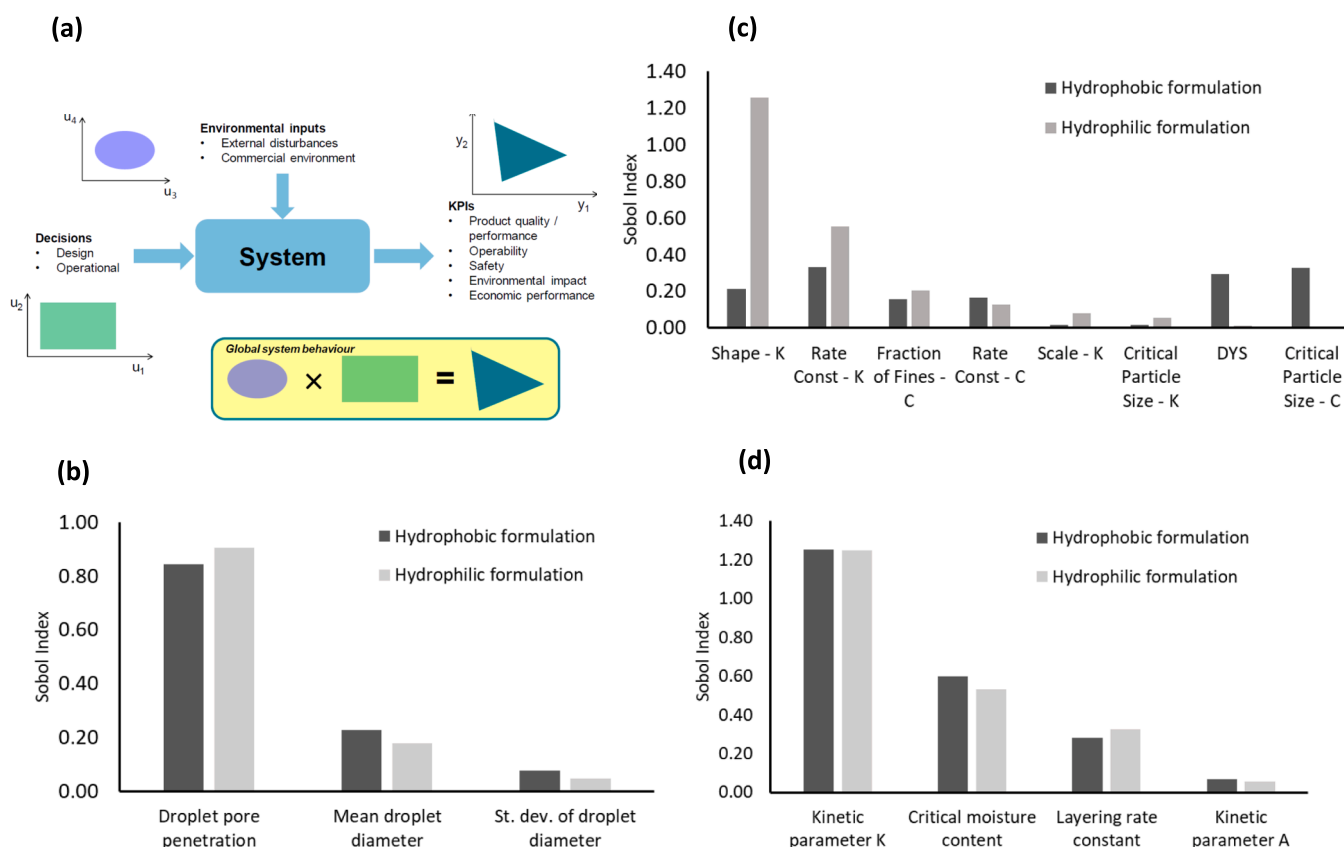
Fig. 3. Average of total effect across D10, D50 and D90 a) GSA schematic to explore input factors and output responses (gPROMS FormulatedProducts 2.2) b) Nucleation c) Breakage (C: Conveying and K: Kneading) d) Layering.

Table 5
Overview of model parameters in the TSG PBM and the method to quantify each one.

Mechanism	4.1.1.1. Input Parameter	Method to Quantify
Nucleation	Mean droplet diameter	Estimate
	St. dev. Of droplet diameter	Estimate
	Droplet pore penetration	Estimate
Breakage	Maximum critical size (x2 – conveying & kneading)	Characterised (screw property) – Literature
	Fitting parameter, a (x2 – conveying & kneading)	Literature
	Fitting parameter, b (x2 – conveying & kneading)	Literature
	Fitting parameter, c (x2 – conveying & kneading)	Literature
	Breakage rate (x2 – conveying & kneading)	Estimate
	Minimum critical size (x2 – conveying & kneading)	Estimate
	Dynamic yield strength (x1)	Estimate
	Proportion of Fines, v	Estimate
	Scale parameter (x3 – 2 conveying & 1 kneading)	Estimate Kneading
	Shape parameter (x3 – 2 conveying & 1 kneading)	Estimate Kneading
Layering	Layering rate constant	Estimate
	Critical moisture content	Estimate
	Kinetic parameter 1 and 2	Estimate
Consolidation	Consolidation rate and Minimum porosity	Literature

compartments 1 is referred to as Location 1 (L1), compartment 3 as Location 3 (L3) and compartment 6 as (L6).

Six experiments for model parameter estimation were used as shown in Fig. 4. More details about the selection of experiments for each compartment is discussed in below sections corresponding to each model.

5.2.1. Compartment 1: Wetting zone

In the wetting zone, only nucleation in isolation (without breakage, layering, or consolidation) was considered and Fig. 6 shows the comparison of predictions of granule size with respect to experimental findings for both hydrophilic and hydrophobic models. A significant shift in particle size distribution (PSD) as compared to input (primary particles) was observed after the wetting of powder in compartment 1. For hydrophobic formulation (HCT), at low L/S ratio levels, bimodal granule size distributions are generally obtained (Fig. 6 a)) which can be explained by the formation of loose, over-wetted agglomerates as granulation liquid is dripped into the granulator barrel (Vercruysse et al., 2015, Verstraeten et al., 2017). As the L/S is increased at the same PFN number, PSDs shift from multi-modal to unimodal as more powder interacts with the granulating liquid (Fig. 6 b). However, for hydrophilic formulation (APAP) when considering nucleation in isolation, consistent unimodal behaviors was observed across all process conditions (Fig. 6 c, d).

The Implemented PBM model which solely focuses on the nucleation rate process while excluding growth and breakage, can successfully capture the overall characteristics observed in particle size distributions. These distributions exhibit a transition from a bimodal distribution to a unimodal distribution as the process conditions shift from a low liquid-to-solid (L/S) ratio to a high L/S ratio for hydrophobic formulation and captures a consistent unimodal behavior for hydrophilic formulation. However, there is a need to improve the accuracy of predictions, particularly around the highest peak in the distributions for hydrophilic formulation and first peak for hydrophobic formulation. Estimated values of nucleation parameters are summarised in Table 6 for both models.
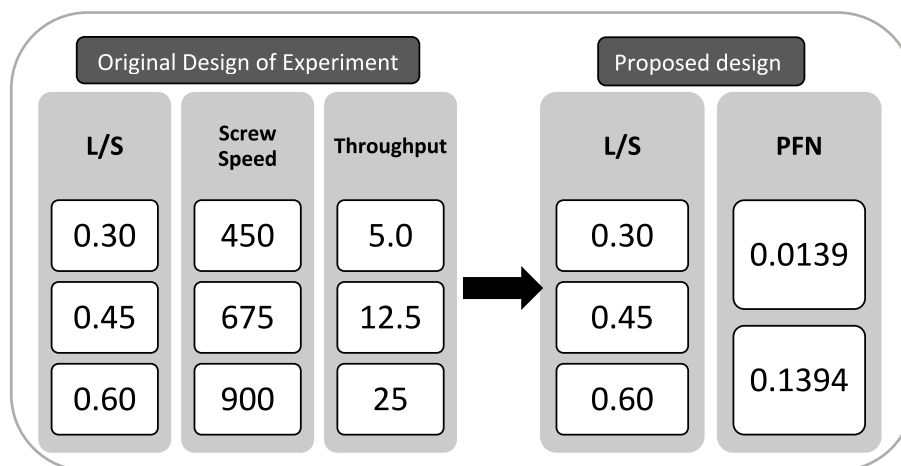
Fig. 4. Proposed experimental design to utilise minimal experimental data for model calibration.
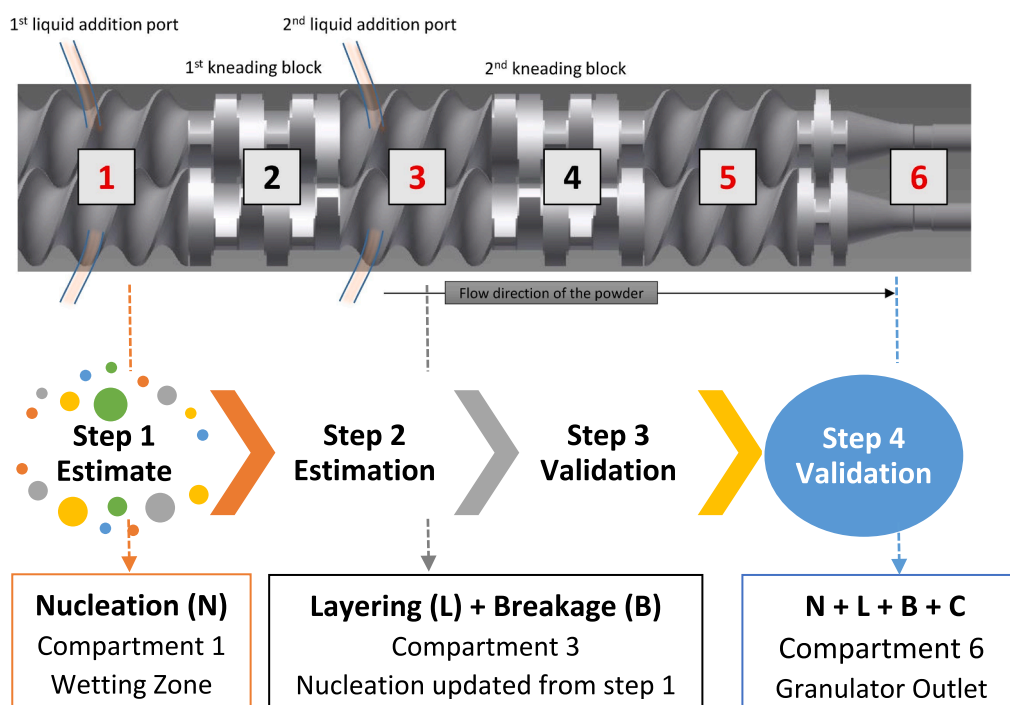

Fig. 5. Approach to parameter estimation.

5.2.2. Compartment 3: After the first kneading compartment

As granules progressed through the first kneading compartment, samples were collected (compartment 3) in Fig. 7. At this stage, the granules undergo all the rate processes (nucleation, breakage, layering and consolidation) simultaneously, dominated by breakage and layering (Wang et al., 2021). In this context, the estimation of layering and breakage parameters takes place using experimental data obtained from Compartment 3 (Fig. 5). Simultaneously, we integrate model input parameters associated with nucleation, which were previously estimated at Compartment 1, where nucleation dominates the mechanism in the wetting zone. Parameters (Breakage and Layering) estimated in this compartment are reported in the Table 7.

For both formulations, as the granules progress from the compartment 1 (L1) to the compartment 3 (L3), the impact of layering becomes evident for both process conditions (Low and High L/S ratio). This was observed as a slight shift in the size distribution tail towards larger sizes (Verstraeten et al., 2017). The model successfully captures the bimodal

nature of the size distribution at the low L/S ratio and the unimodal nature at the high L/S ratio at this location as well. However, it is important to note that further optimization is required to improve the model's performance in accurately representing the behaviours near the highest mode of both distributions. These specific areas of the size distribution require additional refinement to enhance the model's predictive capabilities.

5.2.3. Compartment 6: Granulator outlet

During the transition of granules from compartment L3, which follows the first kneading block, to compartment L5, and then to L6 at the granulator outlet, a notable change in the screw configuration occurs. According to our understanding from relevant literature (Wang Li et al., 2020), several breakage parameters exhibit significant dependence on the screw configuration. As an input, experimental data at granulator outlet (Compartment 6) is utilized here. Although all rate processes were estimated at previous locations, preliminary analysis revealed that re-
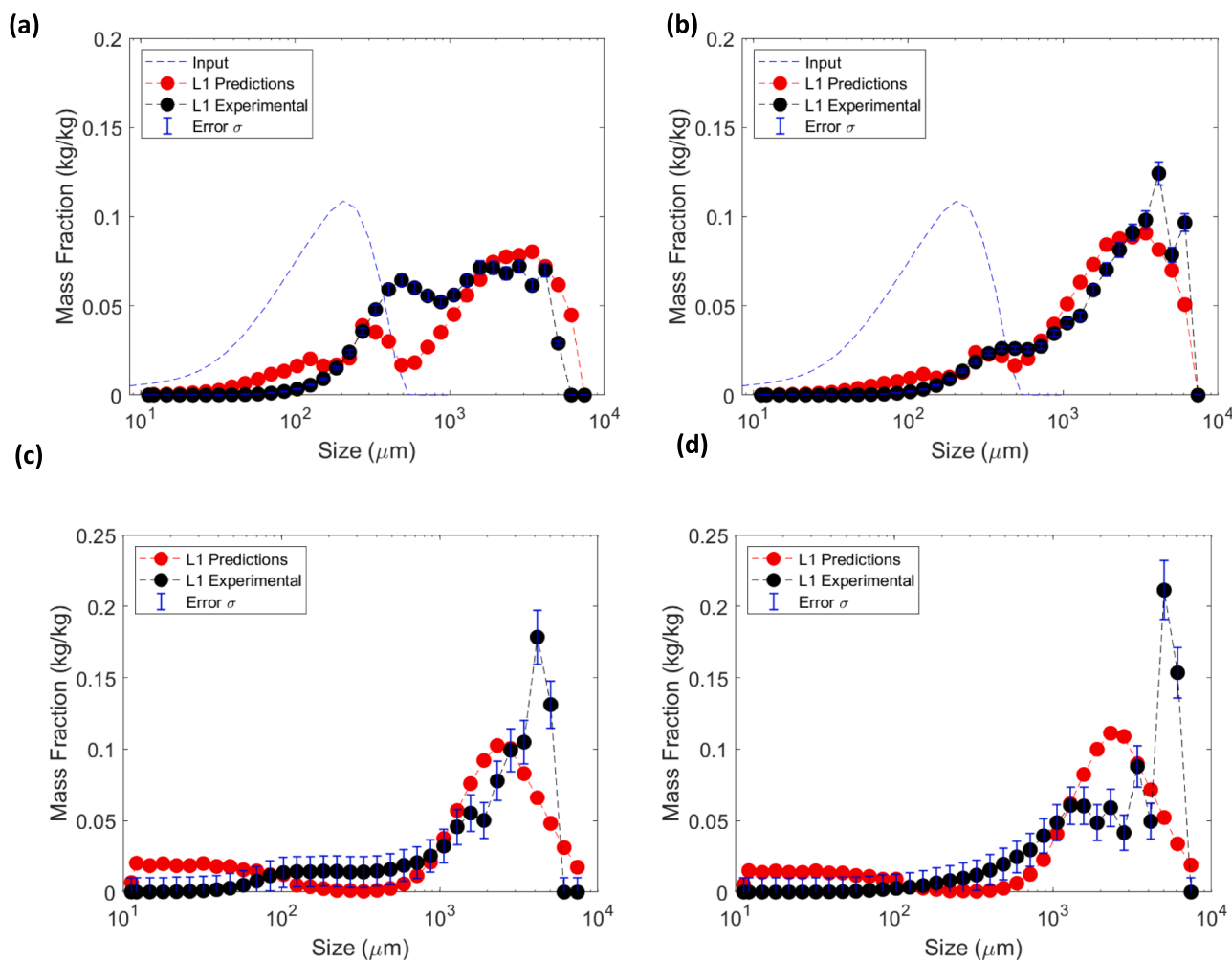
(a)

(b)

(c)

(d)

Fig. 6. Compartment 1- Predictions vs experimental data for granule particle size distribution at PFN = 0.0279 a,b) HCT model at low L/S ratio = 0.3 & high L/S = 0.6 respectively c,d) APAP model at low L/S ratio = 0.408 & high L/S = 0.6 respectively.

Table 6
Nucleation parameter estimated (Compartment 1).

Mechanism	Input Parameter	Method to Quantify	HCT Model	APAP Model
Nucleation	Mean droplet diameter	Estimate	1.12 mm	1.05 mm
	St. dev. Of droplet diameter	Estimate	1.23 mm	0.65 mm
	Droplet pore penetration	Estimate	0.05 m³/m³	0.05 m³/m³

estimating only the certain breakage parameters such as: breakage constant, critical particle size and scale, and shape factor for kneading significantly improved the predictive performance. In addition, due to the hydrophobic nature of the HCT API (Active Pharmaceutical Ingredient), re-estimation of the nucleation parameters was also required. This requirement can be attributed to the limited availability of the granulating liquid. After performing the re-estimation, it was observed that larger droplet size and drop pore penetration were necessary to enhance the predictions. Further investigation is needed to gain a deeper understanding of the re-estimation process for these selected breakage and nucleation parameters. A summary of re-estimated parameters is shown in the Table 8.

Following the passage through the final chopping compartment, which consists of two narrow kneading elements, there is no substantial alteration in the size distribution between compartments L3 and L6 for

the high L/S ratio (Fig. 8 b,d). However, for both formulations, in the case of a low L/S ratio (Fig. 8 a, c), a slight reduction in the size of oversize agglomerates is observed as they undergo breakage, while no noticeable changes are observed in the smaller-sized granules (Verstraeten et al., 2017; Holman, 2013).

6. Model driven workflow

Twin Screw Wet Granulation (TSWG) holds promise in pharmaceutical manufacturing, yet its development requires a structured approach. Building upon our insights from prior sections, we propose a user-friendly workflow integrating a compartmental parameters estimation approach, delineated into six clear steps outlined in user-friendly flowcharts. This methodology serves as a tailored tool for engineers actively engaged in TSWG process development, providing them with a structured framework at each stage. However, it's essential to note that while this framework is proposed, further validation is needed for new formulations within the industry.

In Figure, a model driven workflow is proposed for the twin screw wet granulation model to be used in twin screw process development The workflow is intended to guide a user for the development/use of PBM for the twin screw process by using a mechanistic model driven approach. The workflow consists of 6 stages with 2 Decision points to achieve the overall goal. It can be divided into 2 sections. Stage 1 to 3 where users are required to have prior knowledge about the materials (primary particles and excipients), suitable granulation liquid, and
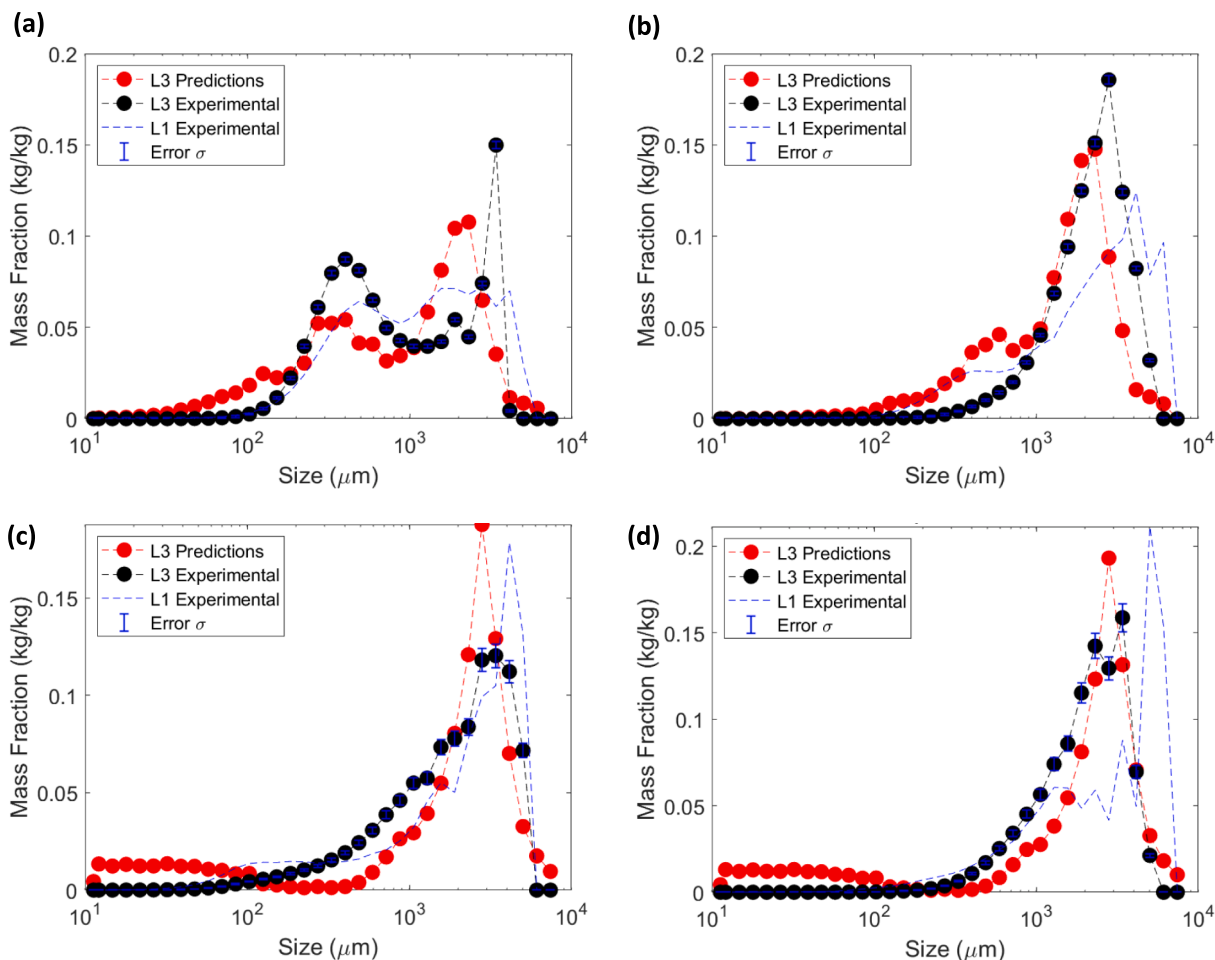
Fig. 7. Compartment 3- Predictions vs experimental data for granule particle size distribution at PFN = 0.0279 a,b) HCT model at low L/S ratio = 0.3 & high L/S = 0.6 respectively c) APAP model at low L/S ratio = 0.408 & high L/S = 0.6 respectively.

Table 7
Layering and Breakage parameter estimated (Compartment 3).

Mechanism	Input Parameter	Method to Quantify	HCT Model	APAP Model
Breakage	Dynamic yield strength	Estimate	4.26 kPa	8.55 kPa
	Fraction of Fines (Conveying)	Estimate	0.090	0.056
	Critical size (conveying)	Estimate	848.65 μm	300.00 μm
	Critical size (kneading)	Estimate	300.00 μm	382.20 μm
	Breakage rate (conveying)	Estimate	3.54 s-1	0.65 s-1
	Breakage rate (kneading)	Estimate	9.16 s-1	3.85 s-1
	Scale parameter (kneading)	Estimate	3.44	1.00
	Shape parameter (kneading)	Estimate	3.57	7.25
Layering	Layering rate constant	Estimate	528.83 μm/s	294.69 μm/s
	Critical moisture content	Estimate	0.53	0.54
	Kinetic parameter A	Estimate	25.000	0.522
	Kinetic parameter K	Estimate	0.08	0.19

Table 8
Breakage and Nucleation parameter re-estimated (Compartment 6).

Mechanism	Input Parameter	Method to Quantify	HCT Model	APAP Model
Breakage	Dynamic yield strength	Estimate	12.43 kPa	10.69 kPa
	Critical size (conveying)	Estimate	614.53 μm	1774.19 μm
	Critical size (kneading)	Estimate	1534.17 μm	507.05 μm
	Breakage rate (conveying)	Estimate	0.10 s-1	1.14 s-1
	Breakage rate (kneading)	Estimate	0.98 s-1	1.07 s-1
	Scale parameter (kneading)	Estimate	1.43	3.00
	Shape parameter (kneading)	Estimate	2.41	1.48
Nucleation	Mean droplet diameter	Estimate	1.28 mm	–
	St. dev. Of droplet diameter	Estimate	0.79 mm	–
	Droplet pore penetration	Estimate	0.13 m³/m³	–

screw geometry specifications.

If all the appropriate information is passed at the first decision point, then the user moves to the next section from Stage 4 to 6. At this stage, users must set up a process model using available experimental data obtained from previous stages, literature and reasonable guesses. Nevertheless, upon reaching Stage 6, initial parameter fitting using the process model can be attempted. Successful fitting and attainment of critical quality attributes within the desired range mark the passage of the final decision point. If insufficient parameter fits are obtained, the
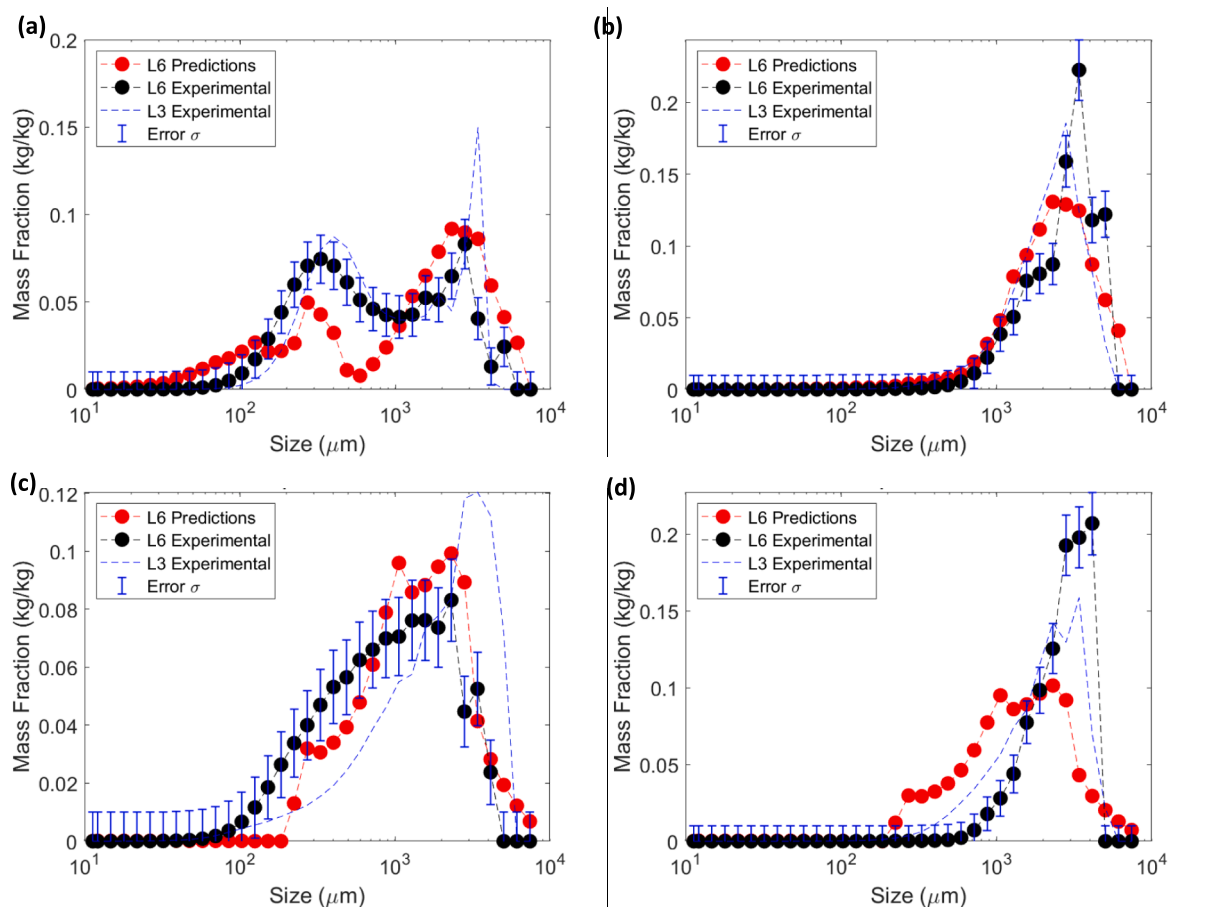
Fig. 8. Compartment 6 (granulator outlet)- Predictions vs experimental data for granule particle size distribution at PFN = 0.0279 a,b) HCT model at low L/S ratio = 0.3 & high L/S = 0.6 respectively c) APAP model at low L/S ratio = 0.408 & high L/S = 0.6 respectively.

user is suggested to further investigate either Stage 4 or section 1 via decision point 2 to investigate the parameter estimation method or available experimental data. In Fig. 9 and Fig. 10, diamond shapes with question mark denote critical decision points that users need to take.

This approach acknowledges that certain aspects relevant to research and development are beyond the scope of the workflow presented. Specifically, the method of generating primary particles is not addressed, and Stage 1 assumes the availability of particles without specifying their generation process. In addition, it should be noted that the workflow assumes the existence of an established population
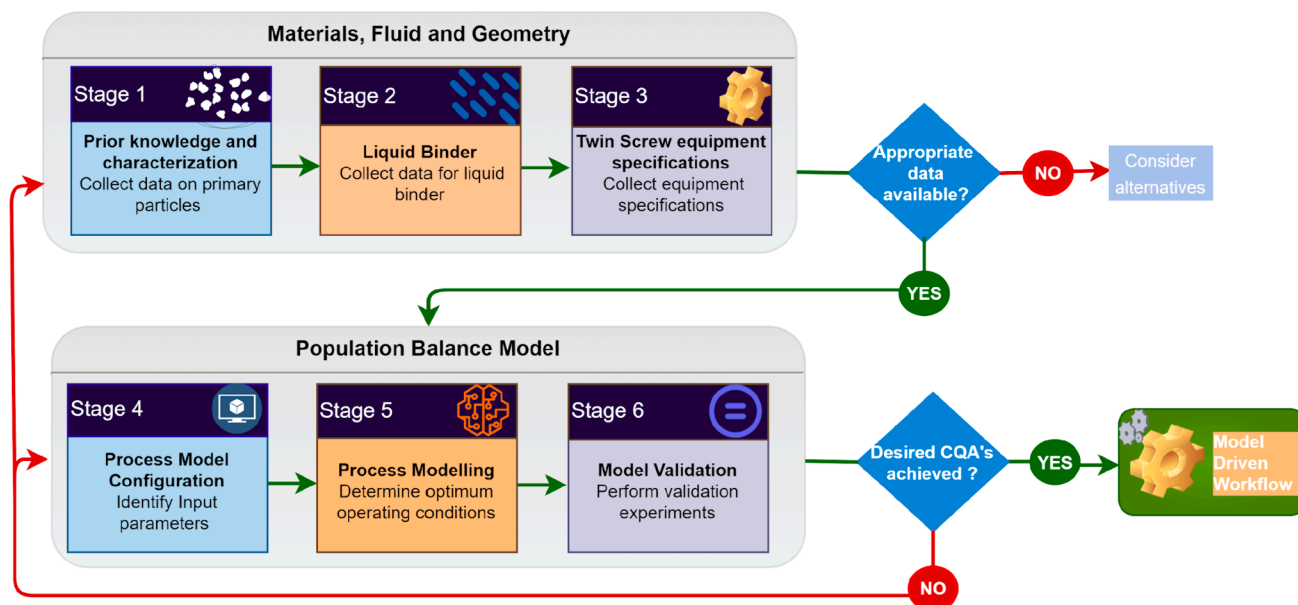

Fig. 9. Model Driven Workflow for TSWG PBM modelling.
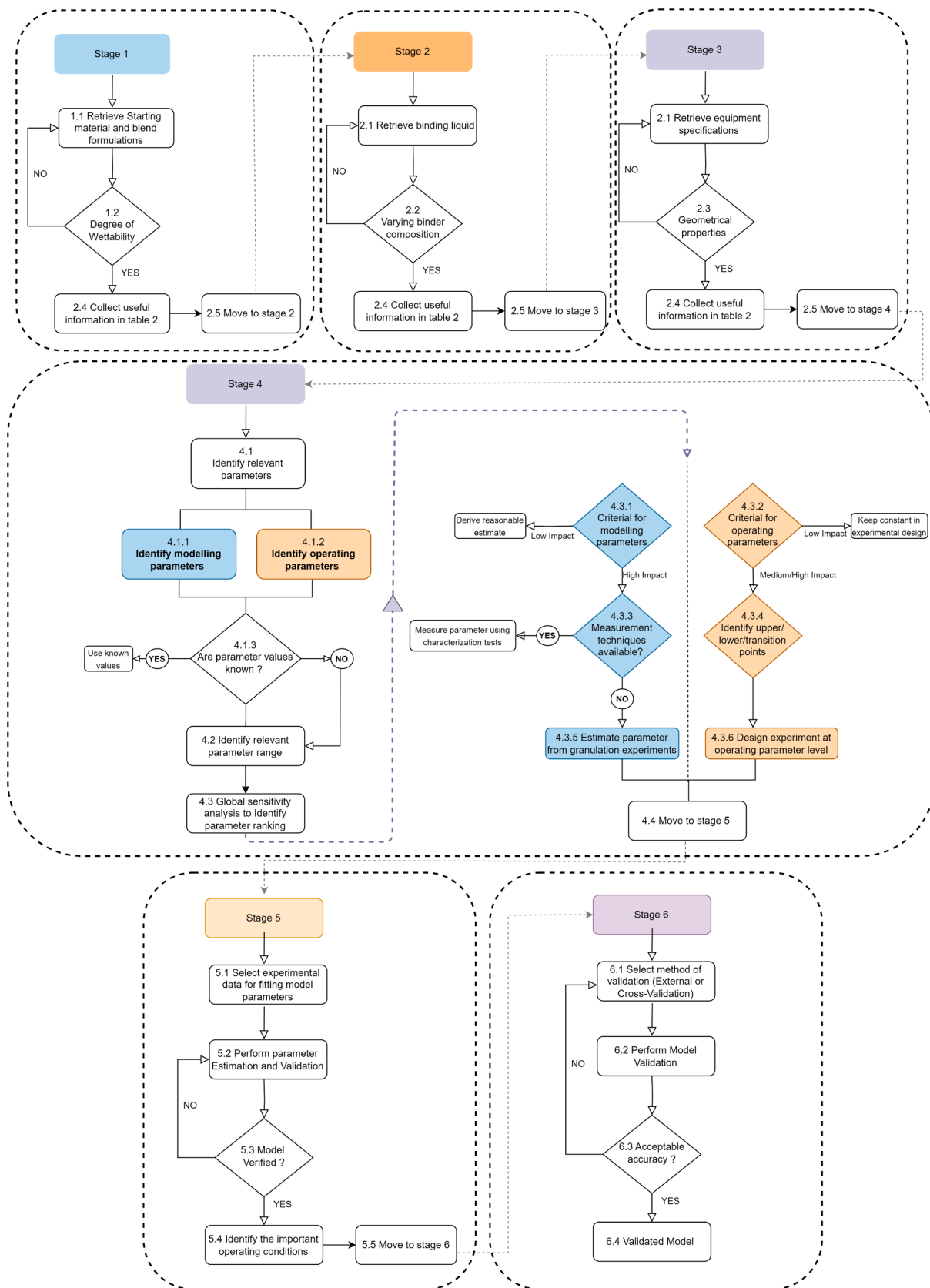
Fig. 10. Schematic flow chart of all stages of the Model Driven Workflow for TSWG PBM modelling.

balance model for the process modelling sections (Stage 4). A process model that incorporates the population balance and relevant mechanistic rate kernels that already exists in gPROMS formulated products has been utilised. Furthermore, the impact of scale-up is not explored in this work. In the following sections, we delve into the specifics of each stage's flow, accompanied by a summary of essential information required to successfully progress through each respective stage.

6.1. Stage 1: Prior knowledge and characterization

Fig. 10 illustrates a flowchart depicting a step-by-step guide for each stage and its interconnection to complete the model-driven workflow. Meanwhile, Table 9 presents a concise summary of crucial information spanning Stages 1 through 3. *Stage 1: Prior Knowledge and Characterisation*, the focus is on gathering essential information about the starting compound (Primary particles). This information might be already available to the user or some initial characterisation is needed if working with new formulations. Currently there is limited availability of literature focusing on the impact of initial properties of primary particles on the critical quality attribution from TSWG. However, the initial essential properties can significantly impact the rate processes such as initial size and wetting properties of primary particles (hydrophilic or hydrophobic).

6.2. Stage 2: Liquid binder

Stage 2 of the workflow involves determining the granulating liquid and its composition. Once the appropriate liquid is selected, the user must then evaluate the wettability of the primary particles. This assessment can be conducted using methods such as the sessile drop method or the Washburn method (Washburn, 1921 & Buckton, 1993). These techniques measure the degree of wettability by analysing the equilibrium contact angle. Based on the obtained equilibrium contact angle, the degree of wettability can be classified into different categories as below.

- Perfect wetting: $\theta = 0^\circ$,
- High wettability: $0^\circ < \theta < 90^\circ$.
- Low wettability: $90^\circ \leq \theta < 180^\circ$.
- Non-wetting: $\theta = 180^\circ$.

Table 9
Priority list of prior knowledge required at Stage 1 to Stage 3 of the workflow.

Stage	Properties	Priority	Method
1	Size & size distribution: Dv10, Dv50, Dv90 and Full PSD	Essential	Size analysis (e.g. diffraction, imaging, sieving)
1	Molecular weight	Essential	–
1	Density (true skeletal density)	Essential	Liquid or gas displacement by solid (e.g. pycnometer)
1	Shape: Volumetric & Surface shape factor	Essential	Shape analysis (e.g. imaging)
1	Contact angle between powder and binding liquid	Essential	Sessile drop method/ Washburn method
1	Polarity	Useful	Literature, Mercury 3D modelling tool
2	Composition	Essential	–
2	Contact angle between powder and binding liquid	Essential	Sessile drop method/ Washburn method
2	Surface tension	Essential	Literature, –
3	Screw element types	Essential	Process
3	Screw configuration: no of elements	Essential	Process
3	Element length (mm)	Essential	Process
3	Mean residence time per length (s/cm)	Essential	Process
3	Screw diameter (cm)	Essential	Process
3	Screw speed (RPM)	Essential	Process
3	Liquid addition port	Essential	Process

These categories help to understanding how effectively the liquid spreads and interacts with the primary particles. By classifying the degree of wettability, users can gain insights into the interfacial behaviour and develop a better understanding of the granulation process. Overall, Stage 2 of the workflow focuses on selecting the granulating liquid and evaluating the wettability of the primary particles, which are crucial factors in the successful implementation of twin screw wet granulation.

6.3. Stage 3: Twin screw equipment specifications

During Stage 3 of the workflow, comprehensive information regarding the specifications of the equipment is collected. This crucial step entails gathering details such as the number of kneading and conveying elements, the length and diameter of the screw, the screw speed, and other relevant parameters. The acquisition of this equipment information is primarily based on process knowledge and the desired quality attributes for the specific application. By considering these factors, researchers can tailor the equipment specifications to optimise the desired outcomes.

6.4. Stage 4: Process model configuration

After identifying a suitable material, fluid, and system geometry through Stages 1 to 3 of the workflow, the focus shifts to Stage 4, where the objective is to configure a process model. This model should encompass appropriate input parameters and conditions, allowing for accurate prediction of granule attributes in the twin screw granulation system. To facilitate this process, a population balance model has been developed and is readily accessible to the user through gPROMS FormulatedProducts (Process Systems Enterprise, Siemens U.K). The first task here is to identify the critical quality attributes that the user would need to model. Typically for twin screw wet granulation, size, full size distribution and porosity would be the most common CQAs. After identifying the quality attributes, the next task will involve the user to configure the relevant parameters including modelling (Stages 4.1.1) as well as operating parameters (Stages 4.1.2). Hence, Stage 4 is divided into two columns: modelling parameters (left) and operating parameters (right). Whenever lines merges within Stage 4, it suggests that same action is required for both modelling and operating parameters, it signifies the integration of steps across both domains. Summary of typical parameters at this stage is discussed including parameters corresponding to different rate processes (Nucleation, Breakage, Layering, Consolidation) and operating parameters (Throughput, Liquid to Solid ratio, Liquid feed rate, Screw Speed). After Stages 4.1.1 and 4.1.2, at first decision point (4.1.3), if user already knows these values which usually comes from prior process knowledge, designed quality attributes and material properties, then user can directly move to Stage 5. For the scope of this work, the range of parameters for two formulations: hydrophilic and hydrophobic explored at different screw configuration are summarised in Table 10 and Table 11 respectively. These values represent a comprehensive summary of all rate parameters estimated in our study using the compartmental approach. These values are proposed as a practical reference starting point for scientists in the twin screw granulation process development field, tailored to the formulation's characteristics. If the API leans towards being more hydrophobic, akin to HCT, then the rate parameter values from Table 10 are recommended as a starting point. Conversely, if it tends towards hydrophilicity, then those from Table 11 are suggested. Operating parameters in twin-screw granulation are typically established through a combination of factors, including experimental design, process knowledge, and the need to balance desired granule characteristics with process efficiency and stability. However, If the model needs to be optimised for new formation whose primary particles are significantly different from APAP and HCT, and there is no prior information on operating parameters available, then step 4.2 and 4.3 in stage 4 should be taken. This includes Identifying relevant parameter ranges followed by conducting a global

Table 10
Reference rate parameters values for hydrophobic type of APIs such as HCT.

Rate	Rate Parameter Input: HCT	L1	L3	L6
Nucleation	Mean droplet diameter	1.12 mm	1.12 mm	1.28 mm
	St. dev. Of droplet diameter	1.23 mm	1.23 mm	0.79 mm
	Droplet pore penetration	0.05 m³/m³	0.05 m³/m³	0.13 m³/m³
Layering	Layering rate constant		528.83 μm/s	528.83 μm/s
	Critical moisture content		0.53	0.53
	Kinetic parameter A		25	25
	Kinetic parameter K		0.08	0.08
Breakage	Dynamic yield strength		4.26 KPa	12.43 KPa
	Fraction of Fines (Conveying)		0.09	0.09
	Critical size (conveying)		848.65 μm	1534.17 μm
	Critical size (kneading)		300.00 μm	614.53 μm
	Breakage rate (conveying)		3.54 s⁻¹	0.10 s⁻¹
	Breakage rate (kneading)		9.16 s⁻¹	0.98 s⁻¹
	Scale parameter (kneading)		3.44	1.43
	Shape parameter (kneading)		3.57	2.41
Consolidation	Consolidation rate	0.002 s⁻¹	0.002 s⁻¹	0.002 s⁻¹
	Minimum porosity	0.2 m³/m³	0.2 m³/m³	0.2 m³/m³

Table 11
Reference values for hydrophilic type of APIs such as APAP.

Rate	Rate Parameter Input: APAP	L1	L3	L6
Nucleation	Mean droplet diameter	1.05 mm	1.05 mm	1.05 mm
	St. dev. Of droplet diameter	0.65 mm	0.65 mm	0.65 mm
	Droplet pore penetration	0.05 m³/m³	0.05 m³/m³	0.05 m³/m³
Layering	Layering rate constant		294.69 μm/s	294.69 μm/s
	Critical moisture content		0.54	0.54
	Kinetic parameter A		0.522	0.522
	Kinetic parameter K		0.19	0.19
Breakage	Dynamic yield strength		8.55 KPa	10.69 KPa
	Fraction of Fines (Conveying)		0.056	0.056
	Critical size (conveying)		300 μm	1774.19 μm
	Critical size (kneading)		382.2 μm	507.05 μm
	Breakage rate (conveying)		3.85 s⁻¹	1.14 s⁻¹
	Breakage rate (kneading)		0.65 s⁻¹	1.07 s⁻¹
	Scale parameter (kneading)		1.0	3.0
	Shape parameter (kneading)		7.25	1.48
Consolidation	Consolidation rate	0.002 s⁻¹	0.002 s⁻¹	0.002 s⁻¹
	Minimum porosity	0.2 m³/m³	0.2 m³/m³	0.2 m³/m³

sensitivity analysis (Elementary or Variance-based) to identify the parameter ranking on the critical quality attributes.

After conducting a global sensitivity analysis concerning both modelling and operating parameters during the workflow, the next step is to categorize the necessary information based on its impact level: low, medium, or high. For modelling parameters with low impact, a reasonable estimate or guess can be derived from existing literature. On the other hand, high impact parameters should be measured using appropriate characterization techniques if available (Stage 4.3.3). If characterization techniques are not available, then at Stage 4.3.5, parameter estimation can be performed using the gPROMS FormulatedProducts software based on granulation experiments (more details in Stage 5). In the experimental setup, operating parameters with low impact can be kept constant, allowing users to focus on identifying the upper, lower, and transition points for the operating parameters that have a significant impact (Stage 4.3.4). These identified points play a crucial role in designing subsequent experiments at Stage 4.3.6. By including these low, high, and transition points in the design of experiments, users can systematically explore the effects of varying operating parameters and their influence on granulation outcomes. This approach enables a comprehensive understanding of how different parameter settings affect the process and provides valuable insights for process optimization and control. Overall, this strategy ensures that the workflow incorporates both existing knowledge and experimental data to obtain reliable estimates for low impact parameters, accurately measure high impact parameters, and effectively explore the operating parameter space for robust experimental design.

6.5. Stage 5: Process modelling

Stage 5 of the workflow aims to thoroughly investigate the configured process model by incorporating the initial experimental data gathered from previous steps for parameter estimation. The primary objective is to enhance the user's process understanding through the utilisation of minimal experiments. By analysing the data within the framework of the process model, important operating ranges can be identified, providing valuable insights into the system's behaviour. The emphasis in this stage is on leveraging the available experimental data to refine and optimise the process model. This iterative process allows the user to gain a deeper understanding of the underlying dynamics and relationships within the system. By adjusting and calibrating the model parameters based on the experimental observations, a more accurate representation of the process model can be achieved.

6.6. Stage 6: Model validation

Stage 6 of the research is focused on the crucial task of validating the Population Balance Model, ensuring that it accurately represents the twin screw wet granulation process for the specific system, taking into account the process conditions within a particular process. The primary objective is to assess the accuracy and reliability of the model's predictions. If the model's predictions at this stage fall outside the acceptable range of accuracy, the user is advised to consider revisiting earlier stages. This may involve going back to Stage 4, which deals with model configuration and parameter estimation. Additionally, it may be necessary to consider improving the input details related to material properties or equipment specifications from Stages 1 to 3. By reevaluating and refining the model in this phase, potential improvements can be made to enhance the accuracy of predictions.

7. Conclusions

This study utilized a population balance model for twin-screw granulators to examine industrial formulations: Hydrochlorothiazide (HCT) and Acetaminophen (APAP). The process model implemented in this analysis integrates pre-existing rate kernels within gPROMS Formulated Products (Siemens Process Systems Enterprise, 2021). Compartmental experimental data provided valuable insights, revealing the impact of model parameters on critical quality attributes. The HCT model successfully captured the transition from bimodal to unimodal particle size distributions at varying liquid-to-solid (L/S) ratios, demonstrating its predictability under different process conditions. Similarly, the model accurately represented the broad unimodal particle

size distributions observed for the APAP blend, showcasing its ability to simulate both formulations.

The study highlighted the effectiveness of the nucleation rate process in isolation, capturing the broad features of particle size distributions for both models and the transition from bimodal to unimodal behavior. Specifically, the nucleation model implemented in the wetting zone effectively portrayed the evolution of the PSD along the granulator's length for the hydrophilic APAP formulation. However, due to the hydrophobic nature of the HCT formulation, re-estimation of nucleation rate parameters was necessary near the granulator outlet, reflecting the unique behavior of the HCT formulation during nucleation. Significant dependencies of breakage rate parameters on material properties and screw configuration, consistent with prior research, led to the re-evaluation of certain parameters within the selection function. Notably, the rate breakage constant and critical size parameter were reassessed, and adjustments were made to the scale and shape parameters exclusively for the kneading blocks. These refined parameters at the granulator outlet enhanced the model's representation of breakage events, leading to improved predictions and a deeper understanding of the granulation process.

A comprehensive model-driven workflow with step-by-step guidelines was proposed. This structured six-step approach provides users with essential details, including flow charts and priority tables, enabling effective utilization of the model for the formulated tests. Reference values for rate parameters (nucleation, layering, breakage, and consolidation) served as a starting point for users to establish appropriate parameter settings based on the specific API characteristics. However, future optimization endeavors could focus on custom modeling the nucleation rate process within gPROMS Formulated Products software (alternatively MATLAB code, COMSOL), allowing detailed analysis of liquid pore penetration and nucleation nature. Additionally, calibrating the model for a broader range of APIs with diverse material properties and formulations could enhance its accuracy and applicability. Notably, the study did not delve into scale-up methodology due to project constraints. Developing a robust scale-up approach stands as a crucial area for further research. Integrating scale-up considerations into the model can provide invaluable insights into the granulation process at larger production scales, enhancing its practical applicability in pharmaceutical manufacturing.

CRediT authorship contribution statement

Neeru Bala: Writing – original draft, Visualization, Validation, Software, Methodology, Investigation, Formal analysis. **Jeremiah Corrigan:** Writing – review & editing, Conceptualization. **Jonathan Meyer:** Writing – review & editing, Conceptualization. **Marek Schongut:** Writing – review & editing, Conceptualization. **Pankaj Doshi:** Writing – review & editing, Methodology, Conceptualization. **Kiran Iyer:** Writing – review & editing. **Kai Lee:** Writing – review & editing, Methodology, Conceptualization. **Martin Rowland:** Writing – review & editing, Conceptualization. **James D. Litster:** Writing – review & editing. **Neil Dawson:** Writing – review & editing, Supervision, Project administration. **Rachel M. Smith:** Writing – review & editing, Methodology, Conceptualization, Project administration, Supervision.

Declaration of competing interest

The authors declare that they have no known competing financial interests or personal relationships that could have appeared to influence the work reported in this paper.

Data availability

Data will be made available on request.

References

Barrasso, D., et al., 2015. Multi-dimensional population balance model development and validation for a twin screw granulation process. Powder Technol. 270, 612–621.

Barrasso, D., Ramachandran, R., 2016. Qualitative assessment of a multi-scale, compartmental PBM-DEM model of a continuous twin-screw wet granulation process. J. Pharm. Innov. 11, 231–249.

Buckton, G., 1993. Assessment of the wettability of pharmaceutical powders. J. Adhes. Sci. Technol. 7 (3), 205–219.

Cameron, I.T., et al., 2005. Process systems modelling and applications in granulation: A review. Chem. Eng. Sci. 60 (14), 3723–3750.

CAMPOLONGO, Francesca, Jessica CARIBONI, and Schoutens WIM. "Enhancing the Morris method." (2005).

Dhenge, R.M., et al., 2012. Twin screw wet granulation: Effects of properties of granulation liquid. Powder Technol. 229, 126–136.

El Hagrasy, A.S., Litster, J.D., 2013. Granulation rate processes in the kneading elements of a twin screw granulator. AIChE J 59 (11), 4100–4115.

Galvis, L., et al., 2022. Retrospective quality by design r (QbD) for lactose production using historical process data and design of experiments. Comput. Ind. 141, 103696.

Gorringe, L.J., et al., 2017. Use of the channel fill level in defining a design space for twin screw wet granulation. Int. J. Pharm. 519 (1-2), 165–177.

Hagrasy, E.l., Arwa, L.G., Wang, Litster, J., 2020. Continuous wet granulation. Continuous Pharmaceutical Processing 269–300.

Holman, J.W. Assessing the use of twin screw wet granulation in a multi stage manufacturing process for the continuous production of pharmaceutical products. University of Surrey (United Kingdom), 2013.

Iveson, S.M., Litster, J.D., Ennis, B.J., 1996. Fundamental studies of granule consolidation Part 1: Effects of binder content and binder viscosity. Powder Technol. 88 (1), 15–20.

Jiménez, A.A.B., et al., 2023, 419,. Model development and calibration of two-dimensional population balance model for twin-screw wet granulation based on particle size distribution and porosity. Powder Technol., 118334

Jiménez, A.A.B., et al., 2023, 640,. Partial least squares regression to calculate population balance model parameters from material properties in continuous twin-screw wet granulation. Int. J. Pharm., 123040

Jiménez, A.A.B., et al., 2023, 193,. Linking material properties to 1D-PBM parameters towards a generic model for twin-screw wet granulation. Chem. Eng. Res. Des. 713–724.

Jiménez, B., Alejandra, A., et al., 2021. Improvement of a 1d population balance model for twin-screw wet granulation by using identifiability analysis. Pharmaceutics 13 (5), 692.

Kumar, A., et al., 2016, 89,. Model-based analysis of a twin-screw wet granulation system for continuous solid dosage manufacturing. Comput. Chem. Eng. 62–70.

Kumar, A., et al., 2016, 90,. Linking granulation performance with residence time and granulation liquid distributions in twin-screw granulation: An experimental investigation. Eur. J. Pharm. Sci. 25–37.

Kumar, A., et al., 2016, 300,. Development of a process map: A step towards a regime map for steady-state high shear wet twin screw granulation. Powder Technol. 73–82.

Litster, J., 2016. Design and processing of particulate products. Cambridge University Press.

Liu, H., et al., 2019. Assessment of spatial heterogeneity in continuous twin screw wet granulation process using three-compartmental population balance model. Pharm. Dev. Technol. 24 (1), 105–117.

Meier, R., et al., 2017. Impact of fill-level in twin-screw granulation on critical quality attributes of granules and tablets. Eur. J. Pharm. Biopharm. 115, 102–112.

Melkebeke, V., Barbara, C.V., Remon, J.P., 2008. Validation of a continuous granulation process using a twin-screw extruder. Int. J. Pharm. 356 (1-2), 224–230.

Mitchell, M., 2014. Determining criticality—process parameters and quality attributes part II: design of experiments and data-driven criticality. BioPharm International 27, 1.

Morris, M.D., 1991. Factorial sampling plans for preliminary computational experiments. Technometrics 33 (2), 161–174.

Osorio, J.G., et al., 2017. Scaling of continuous twin screw wet granulation. AIChE J 63 (3), 921–932.

Peeters, M., et al., 2023. Evaluation of the influence of material properties and process parameters on granule porosity in twin-screw wet granulation. Int. J. Pharm. 641, 123010.

Peeters, M., et al., 2024. Analysis of the effect of formulation properties and process parameters on granule formation in twin-screw wet granulation. Int. J. Pharm. 650, 123671.

Saleh, M.F., et al., 2015. Twin screw wet granulation: Binder delivery. Int. J. Pharm. 487 (1-2), 124–134.

Seem, T.C., et al., 2015. Twin screw granulation—A literature review. Powder Technol. 276, 89–102.

Siemens Process Systems Enterprise. (2021). gPROMS FormulatedProducts (2.2 ed.).

Sobol, I.M., 2001. Global sensitivity indices for nonlinear mathematical models and their Monte Carlo estimates. Math. Comput. Simul 55 (1-3), 271–280.

Thompson, M.R., 2015. Twin screw granulation–review of current progress. Drug Dev. Ind. Pharm. 41 (8), 1223–1231.

Van Hauwermeiren, D., et al., 2019. On the modelling of granule size distributions in twin-screw wet granulation: Calibration of a novel compartmental population balance model. Powder Technol. 341, 116–125.

Vanhoorne, V., et al., 2016. Development of a controlled release formulation by continuous twin screw granulation: Influence of process and formulation parameters. Int. J. Pharm. 505 (1-2), 61–68.

Vercruysse, J., et al., 2015. Impact of screw configuration on the particle size distribution of granules produced by twin screw granulation. Int. J. Pharm. 479 (1), 171–180.

Verstraeten, M., et al., 2017. In-depth experimental analysis of pharmaceutical twin-screw wet granulation in view of detailed process understanding. Int. J. Pharm. 529 (1-2), 678–693.

Wang, H., et al., 2017. A review of process intensification applied to solids handling. Chem. Eng. Process. 118, 78–107.

Wang, L.G., et al., 2020. A breakage kernel for use in population balance modelling of twin screw granulation. Powder Technol. 363, 525–540.

Wang, L.G., et al., 2021. Model driven design for twin screw granulation using mechanistic-based population balance model. Int. J. Pharm. 607, 120939.

Washburn, E.W., 1921. The dynamics of capillary flow. Phys. Rev. 17 (3), 273.